IMPROVEMENTS TO PWR VESSEL FRACTURE ANALYSIS METHODS

A. Pellissier Tanon

Framatome, Tour Fiat, Cédex 16, 92084 Paris La Défense, France

ABSTRACT

The Developments in France aimed at improving the accuracy of the PWR vessel fracture resistance analysis proceed according to two objectives. Every effort is being made to expand the field of applicability of methodologies based on LEFM with plasticity corrections. At the same time, however, a more fundamental elastoplastic numerical approach based on crack tip tearing or cleavage damage criteria is being derived in order to extend the limits of validity of the J integral criterion and to define the limits of validity of the methodology based on LEFM with plasticity corrections.

KEYWORDS

Design, fracture criteria, damage, crack tip, J integral, tearing, cleavage, elastoplastic, plasticity correction, design rule, design code.

1. INTRODUCTION

Article 9 of the "Arrêté dated Feb. 26, 1974", governing the design and construction of PWR Primary Circuits, requires that the resistance to fast fracture be demonstrated for all components forming the primary circuit boundary. The manufacturer is left free to choose the methods but he has to justify them.

This paper presents the development made in France to improve the accuracy of the vessel fracture resistance analysis. The primary piping and other primary component analyses call for the same methods and when necessary for other methods developed elsewhere, such as the net section stress criterion |1|,|27| and the tearing instability approach |2|, both applied to piping, and the two criteria approach |3|, applied to piping and vessels.

2. ESSENTIAL FEATURES OF PWR VESSEL ANALYSIS PROBLEMS

Probabilistic and deterministic approaches have both been considered in the countries developing Pressurized Water Reactors :

- The probabilistic approach is used for risk analyses in view of global safety appraisals, as in |4|.

- The deterministic approach is used either for defining the practical decisions to be taken when defects are found after plant erection or in service, as in |5|, or to assess safety margins at the design stage, as in |6|.

The stringent safety requirements for Nuclear Steam Supply Systems (NSSS) operation has lead the representatives of the French safety authorities to ask for highly reliable data and results. For the deterministic approach this has lead to the notion of conservatism at each stage of analysis. To prevent calculations from becoming excessively pessimistic, it is then necessary to improve the accuracy of data and computational models. As regards input data, the following items have to be considered : type and number of transients as confirmed by operational transient monitoring, variations in toughness properties which are related to variations in as-manufactured metallurgical characteristics and potential radiation effects, and variations in fatigue crack growth rate. A summary of recent works on material properties is given in |7|. As regards computational models, the following parameters must be known : mechanical limits for valid use of the criteria and the degree of accuracy with which the mechanical models can be used to compute the quantities required for expression of the criteria.

Probabilistic analyses of PWR vessel behaviour have given very low fracture probabilities |4||8||9|, thus demonstrating that reactor vessel fast fracture does not constitute a significant part of the overall NSSS operational risks. Meanwhile, the deterministic approach incorporating conservation at each stage of analysis leads in some instances to cases with low safety margins with respect to the chosen criteria. But these cases with low margins have a very low probability of occurence due to the multiplication of the low probabilities affecting each stage of the analysis.

The essential physical features for the analysis of PWR vessels are :

- The large cooldown thermal shock loadings occuring during infrequent incidents requiring operation of the Emergency Core Cooling System or the Residual Heat Removal System which involve large cold water flowrates.

- Irradiation of the part of the vessel closest to the core which leads to evaluation of the risk of initiating cleavage propagation in the embrittled zone at the inner side of the vessel belt-line.

- Use of 18 Cr - 10 Ni type austenitic steels for cladding the vessel internal surface and for buttering and welding of the nozzle safe end which will be welded on site to the primary piping.

The type of manufacturing defects to be considered are mainly lack of fusion or inclusions, in 18-10 SS cladding, buttering and welds or in base metal welds, and under-clad defects such as cold or reheat cracks created during cladding operations or subsequent heat treatments.

The main crack configurations to be considered for the mechanical models are thus :

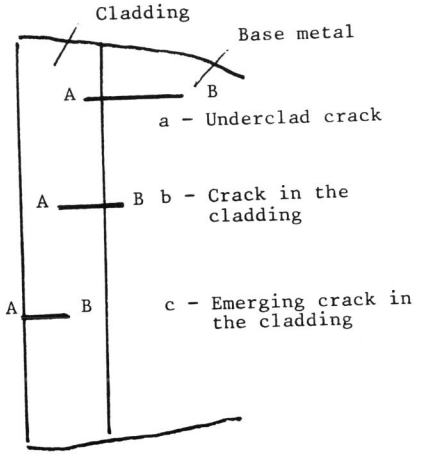

Fig. 1. Cracks near the cladding

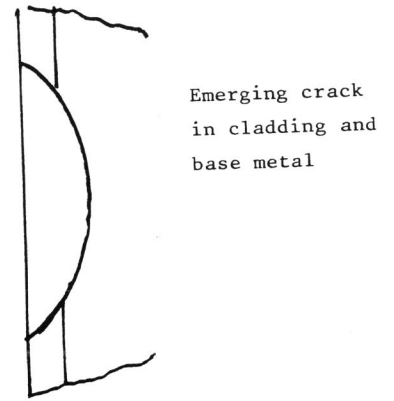

Fig. 2. Emerging crack through cladding and base metal

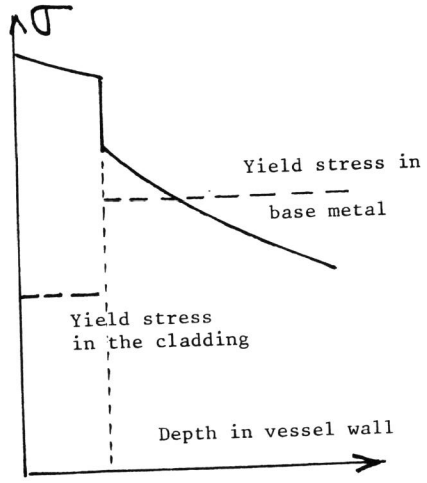

Fig. 3. Stress profile under large LOCA at the belt line

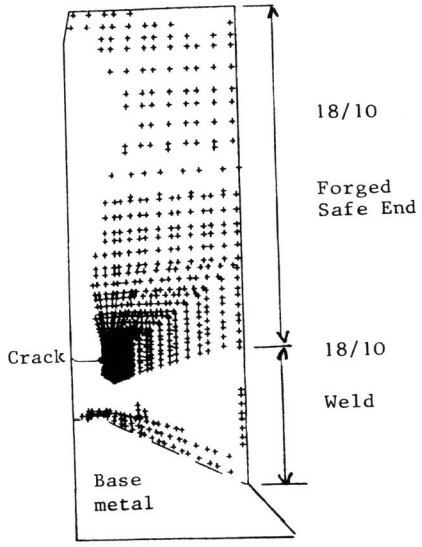

Fig. 4. Plastic deformation of a cracked nozzle safe end under large LOCA

- Underclad cracks with tip A against the cladding or penetrating the cladding after fatigue propagation and tip B in the base metal (Figure 1a).

- Cracks in the cladding with tip B against the base metal or penetrating the base metal after fatigue propagation (Figure 1b).

- Emerging cracks in the cladding outer layer with tip B still in the cladding (Figure 1c).

- The emerging crack resulting from the very unlikely combination of several of the above defects with part of the crackfront in the base metal and part in the cladding (Figure 2).

- Internal defects in base metal welds or base metal repairs.

- Internal or emerging defects in the 18-10 SS parts at the nozzle ends.

During the most severe cooldown thermal shock, the cladding and some adjacent layer of base metal undergo plastic deformation, as well as extended volumes of the austenitic nozzle parts (Figures 3 and 4). However, the fact that the vessel remains globally elastic for most of the transients leads to a condition of contained plasticity for most of the computations, which can therefore be undertaken by Linear Elastic Fracture Mechanics. However, care must be taken to account for the possibility of the ligament between the crack tip and the external surface becoming fully plastic.

The development of analysis methods has been based on the following considerations :

- Rigorous application, wherever possible, of Linear Elastic Fracture Mechanics with plasticity corrections, based on the J integral criterion.

- The development of an elastoplastic approach associated with the definition of crack tip damage criteria in order to analyse cases of generalized plasticity as well as cases for which the J integral cannot be used as a criterion.

3. DEVELOPMENT OF THE METHODOLOGY BASED ON LINEAR FRACTURE MECHANICS WITH PLASTICITY CORRECTION

This approach, already described in |10||11|, consists in estimating the quantity K_J defined from the RICE J integral as $K_J = (EJ/1-\nu^2)^{1/2}$ by the computation of a quantity K_{cp} obtained by applying a plasticity correction to the elastic stress intensity factor K_I.

The starting point is the verification, achieved by several computations, that in small scale yielding, and in plane strain conditions, K_J is very close to the quantity $K_y = K_I[(a + r_y)/a]^{1/2}$, with $r_y = 1/6\pi(K_I/\sigma_y)^2$.

The principle of plasticity correction stems from the discovery that the variation of the ratio K_J/K_y, when the ligament between the crack tip and the free surface becomes fully plastic under increasing load, depends aboveall on the relative extent of the crack tip plastic zone through the ligament. Plasticity correction can therefore be expressed with an acceptable degree of accuracy as a function of the ratio of the quantity $R=1/\pi(K_I/\sigma_y)^2$, which expresses the order of magnitude of the extension of the crack tip plastic wings in small scale yielding, to the width b of the ligament.

Appendix ZG of the PWR Design and Construction Code, RCC-M, proposes the following rule to compute K_{cp} |10|.

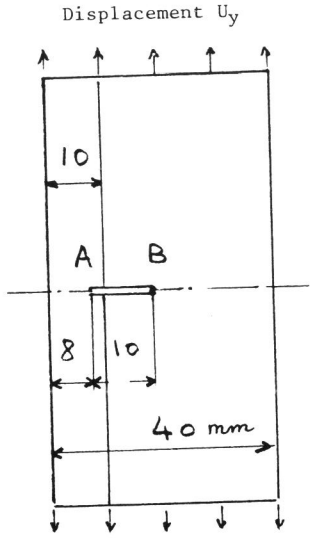

Fig. 5. Bimaterial plate with internal crack.

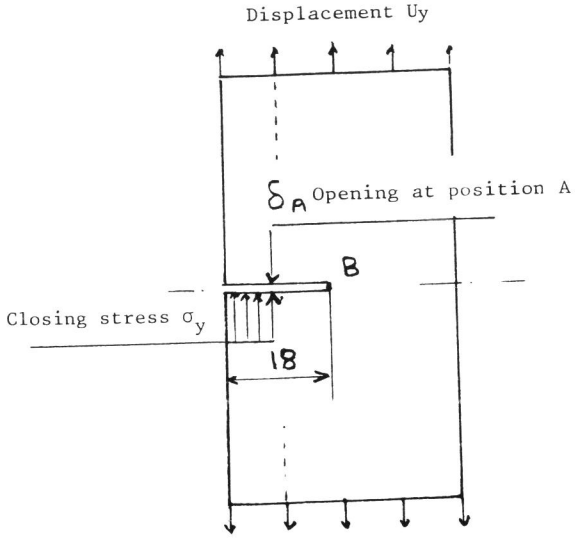

Fig. 6. Same plate with an emerging crack for analysis by the strip yield model.

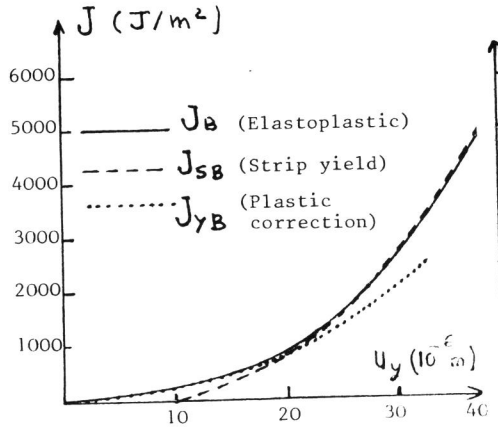

Fig. 7. J at crack tip B

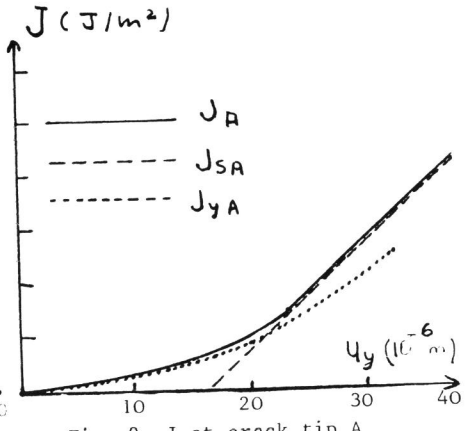

Fig. 8. J at crack tip A

$$\begin{cases} K_{cp} = K_y = K_I \left[(a + r_y) / a \right]^{1/2} & \text{for } R < 0.3\ b \\ K_{cp} = \alpha K_y \text{ with } \alpha = 1 + 0.15 \left(\dfrac{R - 0.3b}{0.2b} \right)^2 & \text{for } 0.3b < R < 0.5b \end{cases}$$

When the ligament at crack tip A reaches the fully plastic state, with $R > 0.5b$, it is possible to account for the effect of the loss of elastic containment at crack tip A on crack tip B, and to obtain a good approximation of J at tip A with the strip yield model, as illustrated by Figures 5 to 8.

Figure 5 presents an internal crack penetrating into the cladding on a plate loaded by a uniform displacement U_y at each end. The cladding is assumed elastic-perfectly plastic with flow stress σ_y and the base metal is assumed elastic (infinite yieldstress). The numerical elastoplastic analysis has given the values J_A and J_B of the J integral at tips A and B as a function of U_y.

Figure 6 presents the model of the same plate with a cut through the cladding analyzed in elastic conditions and subjected to the displacement U_y at its ends and to a normal closing stress σ_y at the non-cracked part of the ligament of the internal crack of Figure 5.

Figure 7, for crack tip B, compares J_B to

$J_{yB} = K_I{}^2{}_B \left[(2a + r_{yA})/2a \right] \left[(1 - \nu^2)/E \right]$, from Figure 5, and to

$J_{SB} = K_I{}^2{}_B \ (1 - \nu^2)/E$ obtained with the model of Figure 6.

General yielding of the ligament at tip A occured for $R_A \simeq 0.5b$; J_{yB} gives a very good approximation of J_B for $R_A < 0.5b$; J_{SB} gives a very good approximation of J_B for $R_A > 0.5b$. If the base metal had been elastoplastic, it may be assumed that the computation of $J_{SB_{cp}} = \alpha^2 K_I{}^2{}_B \left[(a + r_{yB})/a \right] \left[(1 - \nu^2)/E \right]$ with the strip yield model of Figure 6 would have also given a good approximation of J_B when the ligament at tip A is fully yielded but the ligament at tip B remains below general yield.

At tip A, the strip yield model of Figure 6 gives the opening δ_A at the location of tip A, $\delta_A = d_o U_y - \delta_y$ (δ_y is the closing caused by application of σ_y at the ligament of the internal crack of Figure 5).

Figure 8 shows, as expected, that $J_{yA} = K_I{}^2{}_A \left[(2a + r_{yA})/2a \right] \left[1 - \nu^2/E \right]$ is a very good approximation of J_A for $R_A < 0.5b$, and that the quantity $J_{\delta A} = 1.12\ \sigma_y \delta_A$ is a very good approximation of J_A for $R_A > 0.5b$. Actually, the 1.12 coefficient in the expression linking $J_{\delta A}$ to the product $\sigma_y \delta_A$ has been chosen to obtain the best fit, but the finding it can be used simultaneously to fit the slope and the constant factor of the linear relation between J_δ and U_y demonstrates the mechanical soundness of the strip yield model. Other computations and experiments on stainless steel center cracked plates |26|, with ligaments similarly in tension have given a linear relation $J = \beta \sigma_y \delta$ with $\beta \sim 2$. The difference with the preceding value should be accounted for mostly by strain hardening.

4. LIMITATIONS TO THE J INTEGRAL CRITERION AND TO LEFM WITH PLASTICITY CORRECTIONS

The J integral criterion cannot account for the initiation of unstable propagation by cleavage, since numerous toughness measurement programs have revealed a very large influence of specimen size on the value of J at the onset of instable cleavage propagation.

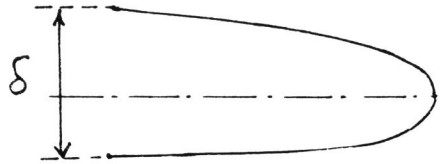

Fig. 9 : Opening profile of crack of Fig. 4 under elastoplastic thermal shock loading.
δ = 0,56 mm at 1,14 mm from the crack tip.

Under thermal loading, the configuration of stresses and strains around the crack tip is not the same as under mechanical loadings, and the opening profile at the crack tip presents a very gradual variation of curvature like the one shown at Figure 9 obtained numerically for a crack at the junction of the austenitic weld to the austenitic safe end during a large loss of coolant accident. A similar result obtained in |12| has been quoted in |11|. This result raises questions about the possible existence of the asymptotic H.R.R. field upon which the J integral criterion is based |13|. It points to the importance of undertaking detailed analyses of the stress and strain fields around the crack tip, and it means that there is no guarantee that the integral modified to remain path independant under thermal loading, computed in |12| and quoted in |11|, has the same meaning in terms of damage at the crack tip as the conventional J integral.

The very gradual variation of curvature at the crack tip makes it also impracticable to use the crack tip opening displacement defined either as a critical opening displacement at a characteristic distance beyond the crack tip or by extrapolating the flanks of the opening profile to a point perpendicular to the crack tip.

On Figure 9, the assymetry of crack profile is due to shear loading components present in the crack plane. Mixed mode loading is an other case for which the meaning, in terms of damage at the crack tip, of the couple J_I-J_{II}, proposed as a substitute to the J integral |14|, is not known.

5. DEVELOPMENT OF A CRITERION FOR DUCTILE TEARING

The development of this ductile tearing criterion and of the cleavage fracture criterion which will be presented in the next paragraph evolves from coordonated studies between the "Laboratoire des Matériaux de l'Ecole des Mines de Paris" under A. PINEAU and F. MUDRY, the "Centre d'Etude des Renardières" of "Electricité de France" under G. ROUSSELIER and the "Centre de Calcul de la Division des Fabrications de Framatome" under J.C. DEVAUX. The achievements at the time of ICF 5 are presented in |15||16||17|. The best review is given in the Doctoral Thesis of F. MUDRY |18|.

The study has been focused on the pressure vessel steel 15 MND6 (A 508 Cl 3). A similar approach is now undertaken for the wrought 316 stainless steel and for 308 SS welds, butterings and claddings.

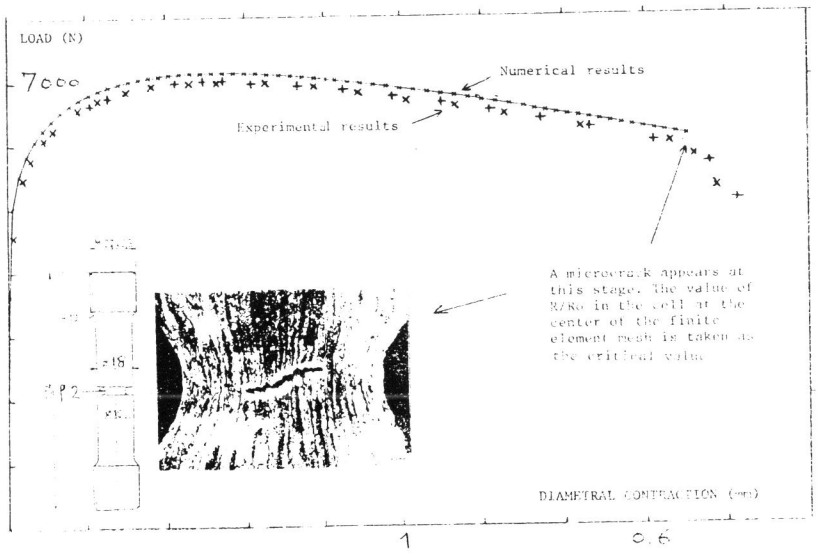

Fig. 10. Determination of $(R/Ro)_c$ with an axisymmetric notched specimen

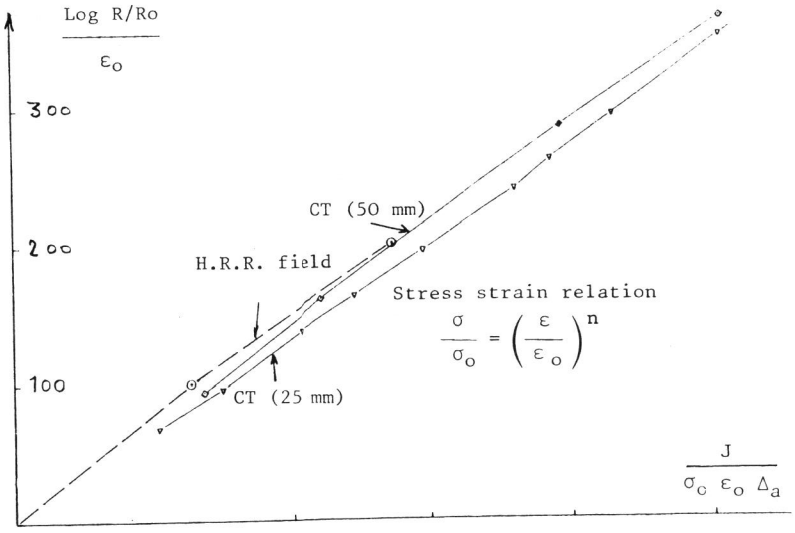

Fig. 11. Correlation between R/Ro, J and Δa on CT specimens

For ductile tearing, the criterion combines :

- A condition for the debonding or breaking of the Manganese Sulphide inclusions :

$$\Sigma + \alpha\,(\sigma_{eq} - \sigma_y) = \sigma_c$$

(Σ is the maximum principal stress, σ_{eq} the equivalent stress, σ_y the yield stress, α and σ_c are material characteristics ; the term $\alpha(\sigma_{eq} - \sigma_y)$ accounts for the effect of the plastic distorsion of the matrix around the inclusions).

- An adaptation of the RICE and TRACEY |19| expression for the rate of growth of cavities :

$$dR/R = 0{,}28\ (d\varepsilon_{eq})\ \exp.\ \frac{3\,\sigma_m}{2\,\sigma_{eq}}$$

(R current radius of the cavity, $d\varepsilon_{eq}$ increment of equivalent strain, σ_m hydrostatic stress, σ_{eq} equivalent stress accounting for strain hardening).

- A critical value $(R/\ell)_c$ or $(R/Ro)_c$ for which the coalescence of cavities is assumed to take place in the analyzed volume, achieving tearing separation. ℓ is the current mean spacing of the cavities, initially distant from ℓ_o ($\ell = e^{\varepsilon_{rr}}\ell_o$, ε_{rr} being the strain in the direction of propagation), R_o is the initial mean inclusion radius.

- A characteristic material volume $(\Delta a_c)^3$ in which the averaging of stress and strain is carried out. Δa_c is related to the mean inclusion spacing $2(N_V)^{-\frac{1}{3}}$, N_V being the number of active inclusions per unit volume. The critical value expressed as $(R/\ell)_c$ or $(R/R_o)_c$ depends of course on Δa_c.

The validity and the accuracy of the method have been verified by cross-checking the results obtained on axisymmetric cracked specimens of 15, 30 and 50 mm diameter and on 25 and 50 mm thick side grooved CT specimens. Debonding of the inclusions occurs at the early stages of loading and can be neglected. Very consistent results have been obtained for initiation, very similar $(R/Ro)_c$ values being found on all specimens. Figure 10 illustrates how $(R/Ro)_c$ is obtained by the experiment and computation of axisymmetric notched specimens.

A very important result is the ability to express the correlations shown on figure 11 between the reduced factor $L_n(R/R_o)/\varepsilon_o$ and the factors $J/(\sigma_o\varepsilon_o\Delta a_c)$, for plane strain, and $G/(\sigma_o\varepsilon_o\Delta a_c)$ for axisymmetric case (G being the axisymmetric integral M |20| reduced to unit of crack length : $G = M/2\pi R$). These correlations depend on the shape of the specimens but little on their size and on the strain hardening exponent. They enable to link together the expression of toughness by the J-Δ_a resistance curve and the $(R/Ro)_c$-Δa_c approach, and hence, to transfer material toughness data from one set to the other. They offer a means of determining Δa_c by combining the results of a few measurements on notched axisymmetric specimens giving $(R/Ro)_c$, of a few measurements on cracked CT specimens giving J_c, and the measurements of the true stress-strain curve giving σ_o, ε_o and n.

An accurate simulation of propagation requires much care for the definition of Δa_c in a pattern accounting for the large deformations occuring around the crack tip. The node release technique investigated in the preliminary work presented in |21| gives rather good results, but only for a limited

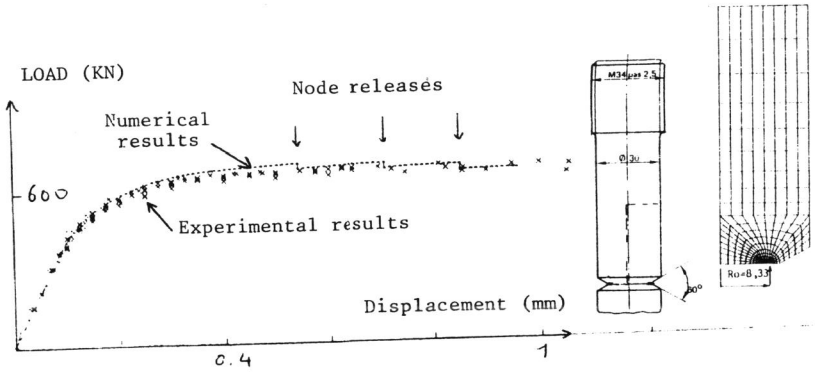

Fig. 12. Numerical simulation of crackgrowth by node releases.

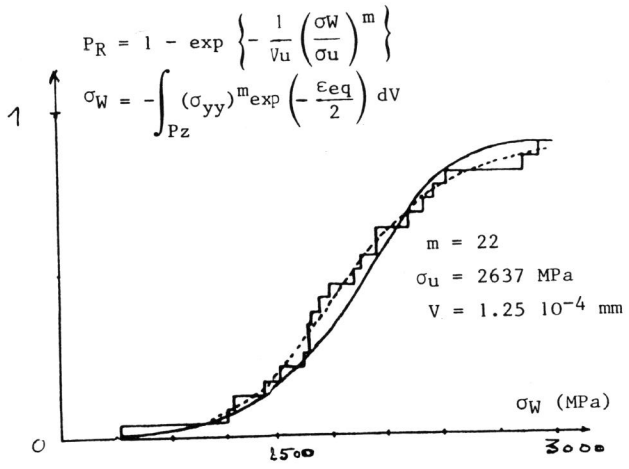

Fig. 13. Probabilistic fit of fracture data on similar notched axisymmetric specimens in a range of sizes from 1 to 4.

amount of propagation, as illustrated by figure 12, applying to a 30 mm diameter axisymmetric specimen. A wider applicability is expected from the approach proposed in |22| in which the expression of the rate of damage undergone by the material affects a strain softening term and a dilatational term in the continuum mechanics expression of the material behaviour. This criterion is now numerically implemented and the report |23| presents the manner in which the numerical factors used in the criterion have been calibrated to obtain an accurate prediction of initiation.

6. DEVELOPMENT OF A CRITERION FOR CLEAVAGE FRACTURE

For cleavage fracture, the criterion expresses the probability of fracture as :

$$P = 1-\exp.\ -\int_{ZP} \left(\frac{\Sigma}{\sigma u}\right)^m \frac{dV}{Vu} \qquad (1)$$

Or :

$$\text{Log}\ (1-P) = \int_{ZP} \left(\frac{\Sigma}{\sigma u}\right)^m \frac{dV}{Vu} \qquad (2)$$

In this expression, the integration is carried out in the volume of the plastic zone ZP, Σ is the maximum principal stress in the volume element dV, and σu, m, Vu, are material characteristics which have been shown to depend slightly or negligibly on temperature.

This criterion has been checked on a series of new experiments performed at - 196°C on notched and cracked axisymmetric and CT specimens, the characteristics factors σu, m, Vu, being determined to obtain the best fit to the experiments.

The manner in which a set of experimental results, obtained on axisymmetric specimens with different notch radii, from 1.3 to 13.3 mm, is processed to determine the material characteristics σu, m, Vu, is illustrated by Figure 13. In this work, the behaviour of the smallest axisymmetric specimens, for which cleavage fracture occured after very large overall plastic deformation, could be fitted to the behaviour of the largest one only by accounting for a negative influence of the plastic strains which can be attributed to micro crack blunting and the shrinkage of grain size in the radial direction under the radial compressive strain.

For small scale yielding, and for a unit length of crack front, the volume dV associated with a given value of Σ varies proportionaly to $(K_I/\sigma_y)^4$. This result makes it possible to derive formulas to account for variations in the level of K_I or in temperature (through its influence on σ_y) or in the size and number of specimens in an experimental program. This approach gives a fairly accurate account of the K_{Ic} scatterband in the transition region, as shown by figure 14. However, attempts to establish a fit to the K_{Ic} scatterband in the lower part of the transition region, assuming σu, Vu, m independent of temperature, showed the need to introduce a threshold value of strain below which cleavage could not take place.

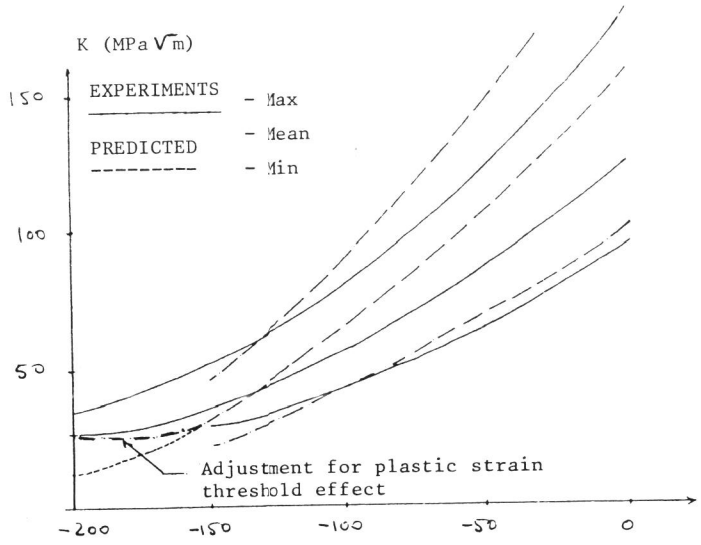

Fig. 14. Prediction of CT specimens behaviour from the data of Fig. 14.

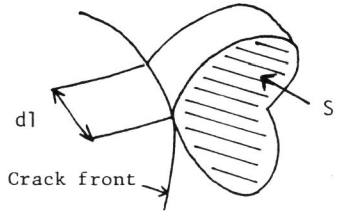

Fig. 15. Coordinates for cleavage criterion in small scale yielding.

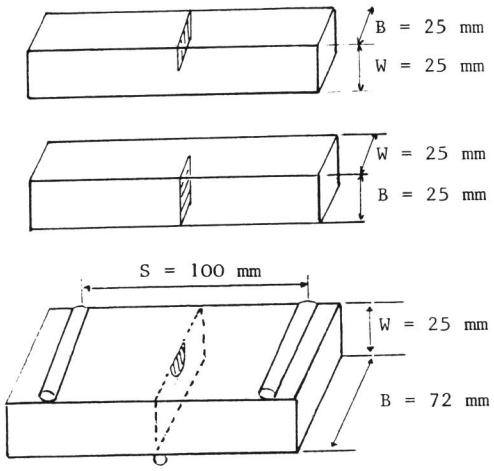

Fig. 16. Shape and size of specimens

The physical reality of this threshold effect has also been disclosed by direct statistical interpretation of the J_c data obtained in large conventional test programs |24|. Similarly, attempts to apply the small scale yielding statistical approach to relate the toughness measured at onset of cleavage instability in the thermal shock experiment |25| to the toughness obtained on the same forging by valid K_{Ic} CT specimens have also shown the threshold effect.

7. APPLICATION AND VERIFICATION OF THE CLEAVAGE CRITERION IN SMALL SCALE YIELDING

Along the front of any crack of complex shape in a complex stress field in mode I loading, the probabilistic cleavage criterion can be written, following the coordinates of figure 15, as :

$$\text{Log } (1-P) = -\int_{ZP}\left(\frac{\Sigma}{\sigma_u}\right)^m \frac{dV}{Vu} = \int_l\int_S\left(\frac{\Sigma}{\sigma_u}\right)^m \frac{1}{Vu}\, dl\, dS$$

For contained plasticity, the surface element dS to which a given value of Σ must be attributed varies proportionally to the square of the characteristic length $(K_I/\sigma_y)2$, therefore :

$$\int_S\left(\frac{\Sigma}{\sigma_u}\right)^m \frac{I}{Vu}\, dS = \alpha\left(\frac{K_I}{\sigma_y}\right)^4$$

$$\text{Log } (1-P) = \int_l \alpha\left(\frac{K_I}{\sigma_y}\right)^4 dl$$

A verification of this expression is given by the interpretation of the results of a program in which bend specimens with fatigue precracked semi-elliptical cracks and prismatic bars taken in the same 15 MND 6 forging, according to figure 16, have been broken at several temperatures in the transition region.

The values of K_I at edge K_{Ib} and deepest point K_{If} computed at fracture for the bend specimens are compared with the K_I at fracture on the prismatic bars, called K_{Ip}, in figure 17. Some averaging must be clearly taken into account to express a fracture criterion, and the experimental averaged ratios K_{If}/K_{Ip} and K_{Ib}/K_{Ip} for the mean values and for the lower bounds are given in table 1.

The values computed for K_I along the front of the semielliptical cracks of the bend specimens can accurately be expressed according to a parabolic expression of the elliptical angle Φ

$$K_I(\Phi) = K_{If} + (K_{Ib} - K_{If})(2\Phi / \pi)^2$$

Hence, for the same probability of fracture, the following relation can be derived between K_{Ip}, K_{If} and K_{Ib} :

$$K_{I_p}^4 B = \int_{-\frac{\pi}{2}}^{+\frac{\pi}{2}} \left[K_{If} + (K_{Ib} - K_{If})\left(\frac{2\Phi}{\pi}\right)^2\right]^4 \left(a^2 \sin^2\Phi + c^2 \cos^2\Phi\right)^{1/2} d\Phi$$

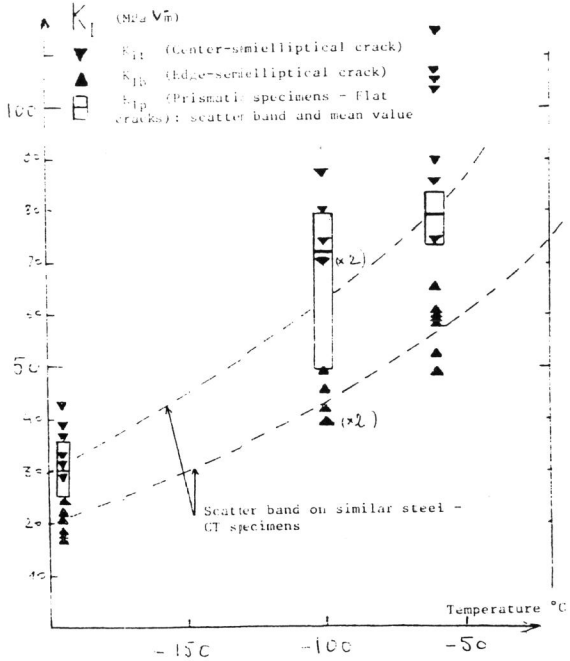

Fig. 17. Behaviour of bend specimens of Fig. 16

Experimental Results						Prediction Probabilistic Criterion
Temperature (°C)	- 196	- 100	- 60	Mean among temperatures	General mean value	
$\frac{K_{Ib}\ mean}{K_{Ip}\ mean}$	1,19	1,06	1,30	1,19	1,22	1,15
$\frac{K_{Ib}\ min}{K_{Ip}\ min}$	1,11	1,43	1,16	1,24		
$\frac{K_{If}\ mean}{K_{Ip}\ mean}$	0,66	0,59	0,72	0,66	0,67	0,65
$\frac{K_{If}\ min}{K_{Ip}\ min}$	0,64	0,59	0,65	0,69		

Table 1. - Mean and minimal experimental values of toughness determined at each temperature, general experimental mean values and prediction of probabilistic criterion.
(K_{Ib} = K_I at edge, K_{If} at center, K_{Ip} = K_I prismatic specimens)

For the range of shape and size of the semielliptical cracks in the bend plates, K_{Ib}/K_{If} = 1.77 , and the interpretation of the above equation leads to :

$$K_{Ib} / K_{Ip} = 1.15 \quad , \quad K_{If} / K_{Ip} = 0.65$$

The very good agreement with the experimental values supports the validity of the probabilistic cleavage criterion.

In practice, if a K_{Ic} reference curve has been established as a safe lower bound to the measurements made on plane specimens with thicknesses as large as Br, an acceptable safe cleavage criterion in small scale yielding is :

$$\int_1 \left(\frac{K_I}{K_{Ic}}\right)^4 dl \leqslant Br$$

where K_{Ic} is the reference toughness for the temperature and the level of irradiation at the point considered along the crack front.

Such a criterion can be used to analyse the margin with respect to the initiation of cleavage fracture for the configuration of figure 2, provided small scale yielding prevails.

8. CONCLUSION

A great deal of research effort is being devoted to the extension of the field of applicability of the methodologies based on LEFM with plasticity correction. At the same time, however, the more fundamental elastoplastic numerical approach based on crack tip tearing or cleavage damage criteria is being derived in order to analyze all cases, particularly those with thermal and mixed mode loadings, for which the validity of the J integral criterion is not demonstrated, and in order to help in defining the limit of applicability of the methodology based on LEFM with plasticity corrections.

9. ACKNOWLEDGEMENT

Support given by Service Central de Sûreté Nucléaire, by Département des Analyses de Sûreté du Commissariat à l'Energie Atomique, by Direction du Développement Scientifique et Technologique du Ministère de l'Industrie et de la Recherche, and by Direction de l'Equipement d'Electricité de France, for several parts of the programs presented is gratefully acknowledged.

REFERENCES

|1| KIEFNER, J.F. and others, in Fracture Toughness, ASTM - STP 536, 461-481, 1973.
|2| PARIS, P.C., and others, in Elastic Plastic Fracture, ASTM - STP 668, 5-36, 1979.
|3| CHELL, G. and MILNE, I., in Elastic Plastic Fracture, ASTM - STP 803, Vol. 2, 179-205, 1983.
|4| DUFRESNE, J., in Advances in Fracture Research, Vol.2, 517 - 532, 1981.
|5| GONNET, B. and others, Revue Générale Nucléaire, 4, 1981, 330 - 336.
|6| BUCHALET, C. and others, SMIRT 6 Post Conference Seminar 6, Assuming Structural Integrity of Steel Reactor Pressure Boundary Components, August 1983.
|7| PELLISSIER TANON,A. and others, in Reliability of Reactor Pressure Components, IAEA, 1983, 255 - 258.
|8| MARSHALL, W., An Assessment of the Integrity of PWR Pressure Vessels, UKAEA, 1976.
|9| STROSNIDER, T.R., Presentations at the 4th US Nat. Congres on Pressure Vessel and Piping, June 1983.
|10| RCC-M, Design and Construction Rules for Mechanical Components of PWR Nuclear Island, 1983, AFCEN, PARIS.
|11| PELLISSIER TANON, A., in Int. Conf. on Applic. of Fract. Mech. to Materials and Structures, Freiburg, June 1983.
|12| CHEISSOUX, J.L., IVARS, J.F., Revue Française de Mécanique, 3, 1983, 15 - 24.
|13| HUTCHINSON, J.W., PARIS, P.C., ASTM STP 668, 1979, 37 - 64.
|14| KISHIMOTO, K., Eng. Fract. Mech., 13, 1980, 841 - 850.
|15| PINEAU, A., in Advances in Fracture Research, Vol. 2, 1981, 553 - 580.
|16| BEREMIN, F.M., in Advances in Fracture Research, Vol. 2, 1981, 809 - 816.
|17| BEREMIN, F.M., in Advances in Fracture Research, Vol. 2, 1981, 825 - 832.
|18| MUDRY, F., Etude de la rupture ductile et de la rupture par clivage d'aciers faiblement alliés, Doctor Thesis, Université de Technologie de Compiègne, 1982.
|19| RICE, J.R., TRACEY, D.M., J. Mech. Phys. Sol. 17, 1969, 201 - 217.
|20| BUDIANSKI, RICE, J.R., J. Appl. Mech., 40, 1973, P.201.
|21| D'ESCATHA, Y., DEVAUX, J.C., ASTM STP 668, 1979, 229 - 250.
|22| ROUSSELIER, G., in Three Dimensional Constitutive Relations, North Holland, 1981, 331 - 335.
|23| ROUSSELIER, G. and others, in 7th Structural Mechanics in Reactor Technology (SMIRT) Edited by CEC, 1983, Paper G/F 1/3.
|24| Mc CABE, D.E., LANDES, J.D., in 7th SMIRT, 1983, Paper G 2/4.
|25| PELLISSIER TANON, A. and others, in 7th SMIRT, 1983, Paper G/F 1/8.
|26| GARCIA, J.L. and others, in 7th SMIRT, 1983, Paper G/F 2/6.
|27| KANNINNEN, M.F. and others, Mechanical Fracture Predictions for Sensitized Stainless Steel Piping with Circumferential Cracks, EPRI, NP-192, 1976.